

**Electronic Supplementary Information for**

**Anodic hydrazine oxidation assisted hydrogen evolution over bimetallic RhIr  
mesoporous nanospheres**

Mei Zhang, Ziqiang Wang\*, Zhongyao Duan, Shengqi Wang, You Xu, Xiaonian Li,

Liang Wang\* and Hongjing Wang\*

State Key Laboratory Breeding Base of Green-Chemical Synthesis Technology, College of  
Chemical Engineering, Zhejiang University of Technology, Hangzhou 310014, P. R. China.

\*Corresponding authors: Ziqiang Wang; Liang Wang; Hongjing Wang

E-mails: zqwang@zjut.edu.cn; wangliang@zjut.edu.cn; hjw@zjut.edu.cn

**Electrochemical measurements:** The electrochemical experiments were performed in a standard three-electrode system. Graphite rod and Hg/HgO electrode were used as the counter electrode and reference electrode in alkaline solution, respectively. For the fabrication of working electrodes, catalysts (2 mg) was dispersed in 1 mL of mixed solution containing 800  $\mu$ L isopropanol, 200  $\mu$ L H<sub>2</sub>O to form a homogeneous catalyst ink. After sonication for 1 h, 5  $\mu$ L of catalyst inks were loaded onto a glassy carbon electrode (GCE) with 3 mm in diameter and dried at room temperature, further coating 3  $\mu$ L of Nafion (0.5 wt %). The electrochemical tests for the overall hydrazine electrolysis were performed in 1.0 M KOH as the cathode electrolyte and 1.0 M KOH/0.5 M N<sub>2</sub>H<sub>4</sub> as the anode electrolyte. Before electrocatalytic experiments, the electrolyte was bubbled by N<sub>2</sub> gas for 30 min. The polarization curves were recorded by linear sweep voltammetry (LSV) at a scan rate of 5 mV s<sup>-1</sup> with *iR* compensation. For *iR* compensation, the uncompensated ohmic resistance value for each electrode in the electrolyte solution was measured. The potential was based on *iR* correction using the equation:  $E(iR\text{-corrected}) = E - iR$ , where *i* is the current and *R* is the uncompensated electrolyte ohmic resistance measured by electrochemical impedance spectroscopy. All potentials were recorded with respect to RHE. The double layer capacitance ( $C_{dl}$ ) was acquired from the cyclic voltammetry (CV) at different scan rates from 20 to 120 mV s<sup>-1</sup>. Electrochemical impedance spectroscopy (EIS) investigations were recorded in the frequency range from 100 kHz to 0.1 Hz at -0.8 V. Faradaic efficiency (FE) for the HER was determined using  $FE = n/(Q/2F)$ ,<sup>[1]</sup> where F is the Faraday constant, n is the total amount of H<sub>2</sub>, and Q is the total amount of charge obtained by the *i-t* curve at voltage of 0.6 V.

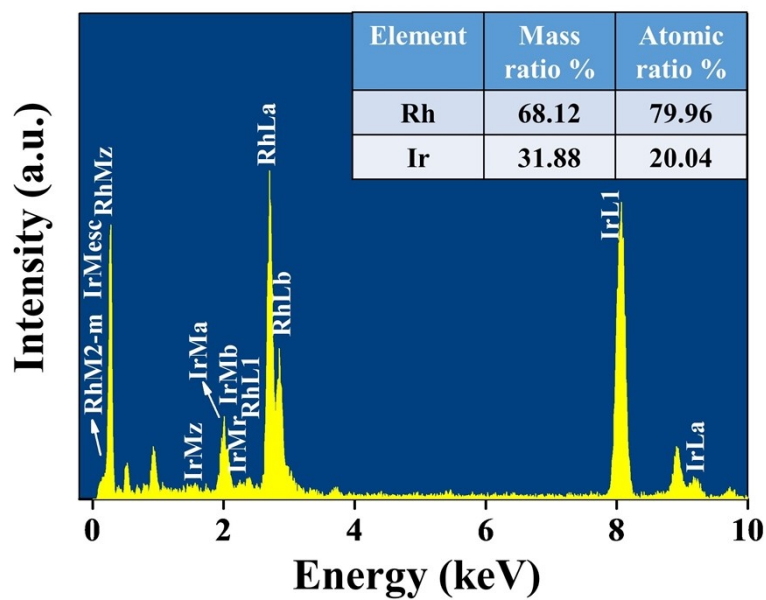


**Fig. S1** EDX spectrum of RhIr MNs.

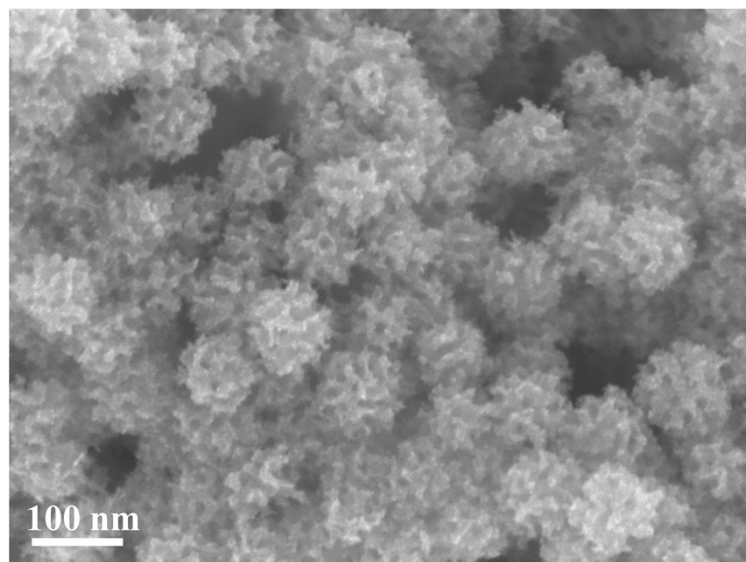


**Fig. S2** SEM image of Rh MNs.

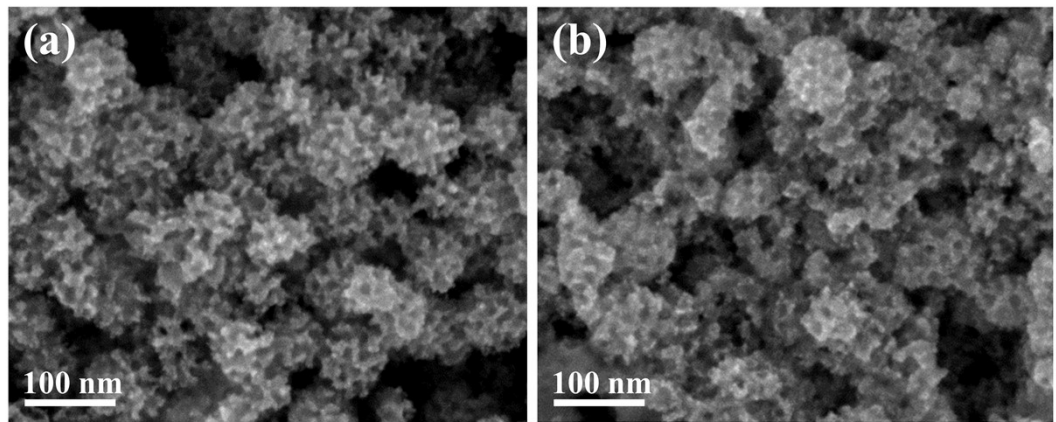


**Fig. S3** SEM images for the samples with different precursor solutions: (a)  $K_3RhCl_6 : IrCl_3 = 3:1$  and (b)  $K_3RhCl_6 : IrCl_3 = 1:3$ .

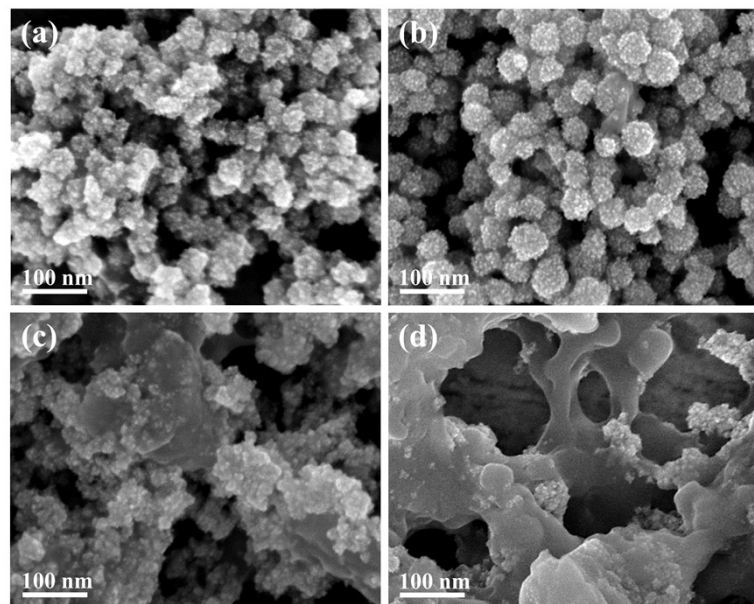


**Fig. S4** SEM images of the samples obtained from different surfactants: (a) F127, (b) Brij 58, (c) CTAC, and (d) PVP.

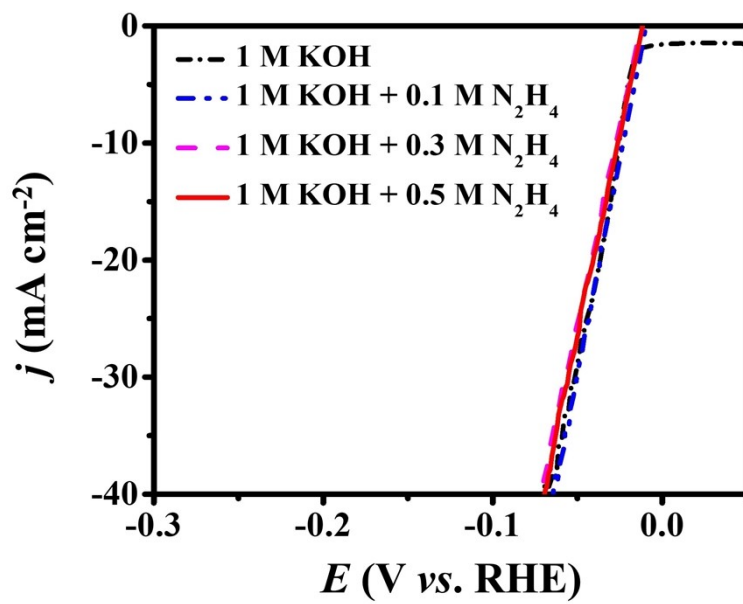


**Fig. S5** HER polarization curves of RhIr MNs in 1.0 M KOH with different concentrations of  $\text{N}_2\text{H}_4$ .

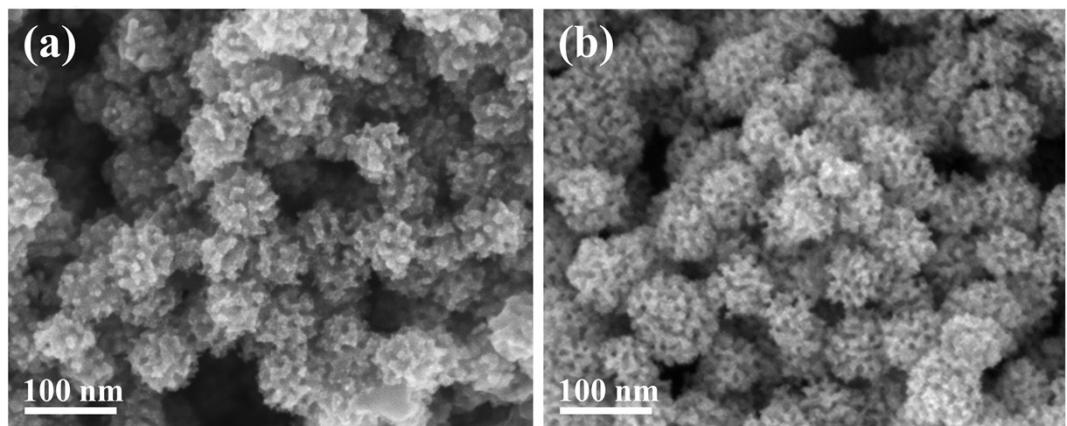


**Fig. S6** SEM images of RhIr MNs after durability tests in (a) 1.0 M KOH and (b) 1.0 M KOH/0.5 M  $\text{N}_2\text{H}_4$ .

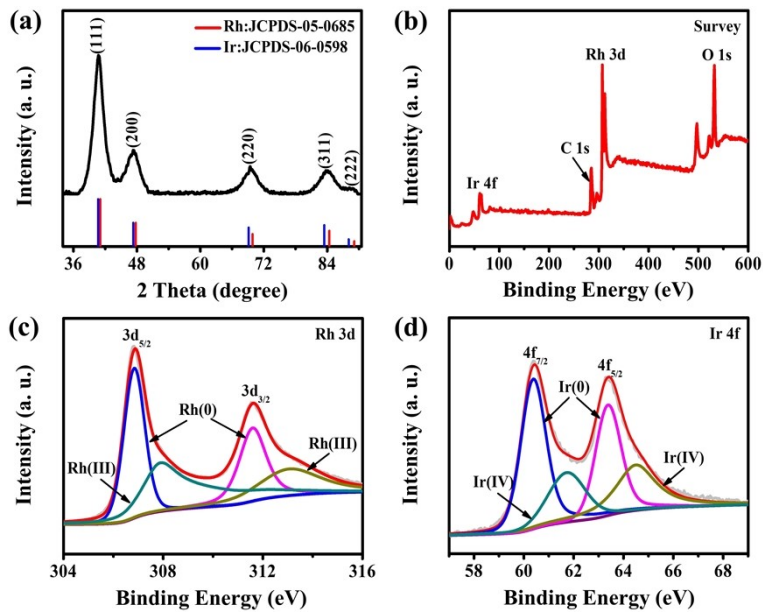


**Fig. S7** Characterizations of post-HER RhIr MNs after durability test in 1.0 M KOH. (a) XRD pattern, (b) XPS survey spectrum, and high-solution XPS spectrum of (c) Rh 3d and (d) Ir 4f.

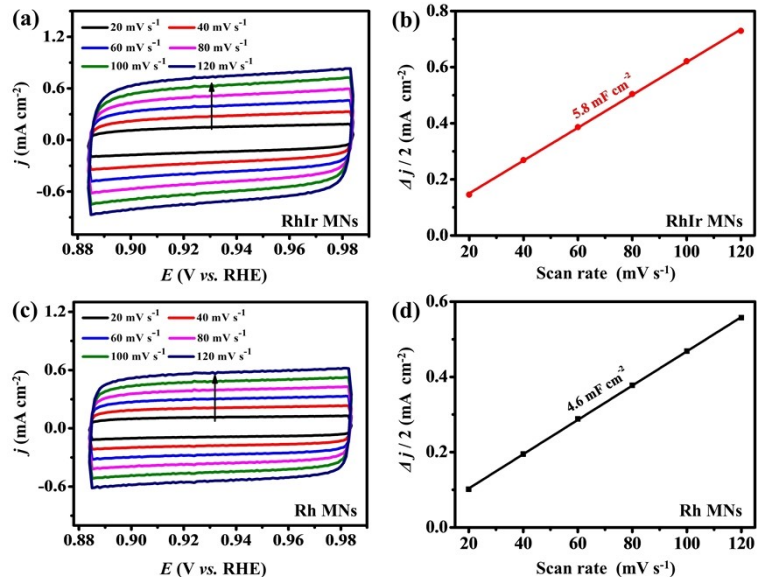


**Fig. S8** CV curves of (a) RhIr MNs and (c) Rh MNs at various scan rates from 0.884 to 0.984 V (vs. RHE) and capacitive current densities of (b) RhIr MNs and (d) Rh MNs in 1.0 M KOH solution.

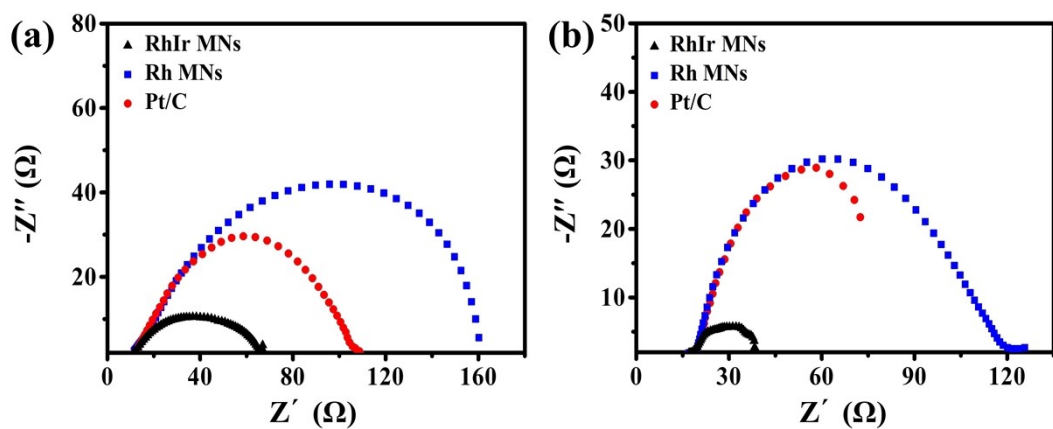


**Fig. S9** EIS spectra of various catalysts for (a) HER in 1.0 M KOH at -0.02 V (vs. RHE) and (b) HzOR in 1.0 M KOH/0.5 M N<sub>2</sub>H<sub>4</sub> at 0.05 V (vs. RHE).

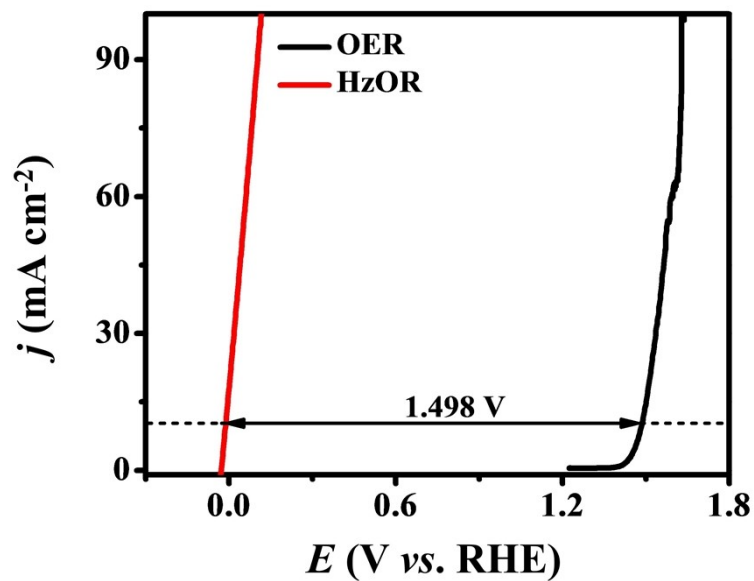


**Fig. S10** Polarization curves of RhIr MNs for OER in 1.0 M KOH and HzOR in 1.0 M KOH/0.5 M N<sub>2</sub>H<sub>4</sub>.

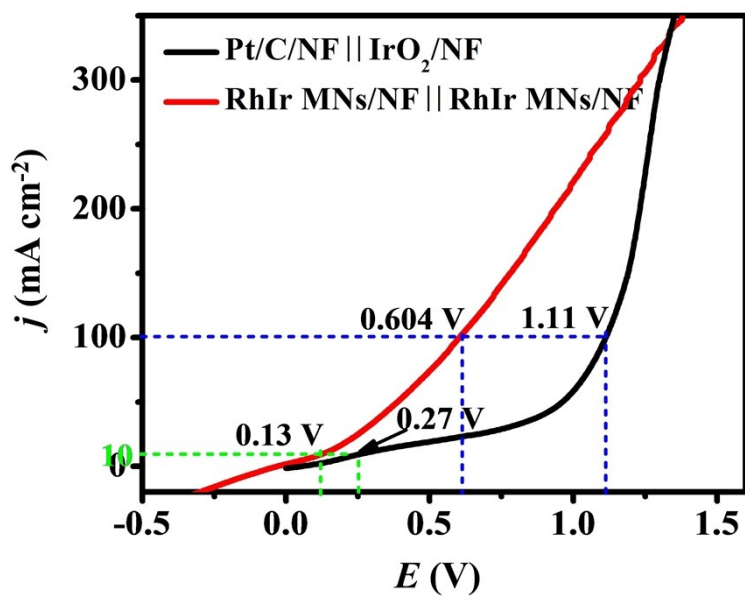


**Fig. S11** Polarization curves for  $\text{RhIr MNs/NF} \parallel \text{RhIr MNs/NF}$  and  $\text{Pt/C/NF} \parallel \text{IrO}_2/\text{NF}$  in overall hydrazine electrolysis.

**Table S1.** HER performance comparison between RhIr MNs and other reported electrocatalysts.

Electrocatalysts	Electrolytes	Overpotential (mV) at 10 mA cm <sup>-2</sup>	Tafel slope (mV dec <sup>-1</sup> )	Ref.
<b>RhIr MNs</b>	<b>1 M KOH</b>	<b>20</b>	<b>30.7</b>	<b>This work</b>
CoSe <sub>2</sub> /MoSe <sub>2</sub>	1 M KOH	168	106.4	1
RhCo-ANAs	1 M KOH	32.4	31.9	2
RhCoB	1 M KOH	43	32.1	3
Rh/Rh <sub>2</sub> P-NFAs.	1 M KOH	19.5	50	4
Rh-Rh <sub>2</sub> P@C	1 M KOH	37	32	5
w-Rh <sub>2</sub> P NS/C	1 M KOH	18.3	61.5	6
RhP <sub>x</sub> @NPC	1 M KOH	69	80	7
Rh <sub>2</sub> P	1 M KOH	30	50	8
Rh NSs	1 M KOH	43	107	9
Rh/N-CBs	1 M KOH	77	74.16	10
Ru-Ru <sub>2</sub> P@NPC	1 M KOH	46	39.75	11
Ni <sub>3</sub> N-Co <sub>3</sub> N	1 M KOH	43	35.1	12
PW-Co <sub>3</sub> N	1 M KOH	41	40	13
Rh <sub>2</sub> S <sub>3</sub> /NC	1 M KOH	38	41	14
Ni NCNA	1 M KOH	47	41	15

**Table S2.** HzOR performance comparison between RhIr MNs and other reported electrocatalysts.

Electrocatalysts	Electrolytes	Potential (V) at 10 mA cm <sup>-2</sup>	Tafel slope (mV dec <sup>-1</sup> )	Ref.
<b>RhIr MNs</b>	<b>1.0 M KOH+ 0.5 M hydrazine</b>	<b>-0.012</b>	<b>30</b>	<b>This work</b>
CoSe <sub>2</sub> /MoSe <sub>2</sub>	1.0 M KOH+ 0.5 M hydrazine	-	142	1
Ni <sub>3</sub> N-Co <sub>3</sub> N	1.0 M KOH+ 0.5 M hydrazine	-0.088	-	12
PW-Co <sub>3</sub> N	1.0 M KOH+ 0.1 M hydrazine	-0.055	-	13
Rh <sub>2</sub> S <sub>3</sub> /NC	1.0 M KOH+ 0.1 M hydrazine	0.095	46	14
Ni NCNA	1.0 M KOH+ 0.3 M hydrazine	-0.026	32.6	15
Cu <sub>1</sub> Ni <sub>2</sub> -N	1.0 M KOH+ 0.5 M hydrazine	0.5	44.1	16
Ni (Cu)@NiFeP /NM	1.0 M KOH+ 0.5 M hydrazine	~0.117	147	17
CoSe <sub>2</sub>	1.0 M KOH+ 0.5 M hydrazine	-0.017	-	18
Ni <sub>2</sub> P	1.0 M KOH+ 0.5 M hydrazine	~-0.065	55	19
NiFe(OH) <sub>2</sub> -SD/NF	1.0 M KOH+ 0.5 M hydrazine	0.06	62	20

**Table S3.** The overall hydrazine splitting performance comparison between RhIr MNs and other reported electrocatalysts.

Electrocatalysts	Electrolytes	substrate	Voltage (V) at 10 mA cm <sup>-2</sup>	Ref.
<b>RhIr MNs</b>	<b>1.0 M KOH+ 0.5 M hydrazine</b>	NF	<b>0.13</b>	<b>This work</b>
CoSe <sub>2</sub> /MoSe <sub>2</sub>	1.0 M KOH+ 0.5 M hydrazine	CC	0.85	1
Ni <sub>3</sub> N-Co <sub>3</sub> N	1.0 M KOH+ 0.5 M hydrazine	NF	0.071	12
PW-Co <sub>3</sub> N	1.0 M KOH+ 0.1 M hydrazine	NF	0.025	13
Rh <sub>2</sub> S <sub>3</sub> /NC	1.0 M KOH+ 0.5 M hydrazine	CP	0.108	14
Ni NCNA	1.0 M KOH+ 0.3 M hydrazine	NF	0.023	15
Cu <sub>1</sub> Ni <sub>2</sub> -N	1.0 M KOH+ 0.5 M hydrazine	CC	0.24	16
Ni(Cu)@NiFeP/NM	1.0 M KOH+ 0.5 M hydrazine	NF	0.147	17
CoSe <sub>2</sub>	1.0 M KOH+ 0.5 M hydrazine	NF	0.164	18
Ni <sub>2</sub> P	1.0 M KOH+ 0.5 M hydrazine	NF	~0.12	19

## References

1. X. Tang, J. Y. Zhang, B. Mei, X. Zhang, Y. Liu, J. Wang and W. Li, *Chem. Eng. J.*, 2021, **404**, 126529.
2. Y. Zhao, J. Bai, X. R. Wu, P. Chen, P. J. Jin, H. C. Yao and Y. Chen, *J. Mater. Chem. A*, 2019, **7**, 16437-16446.
3. K. Deng, T. Ren, Y. Xu, S. Liu, Z. Dai, Z. Wang, X. Li, L. Wang and H. Wang, *J. Mater. Chem. A*, 2020, **8**, 5595-5600.
4. Y. Q. Yao, Z. J. Wang, R. L. Zhang, L. Zhang, J. J. Feng and A. J. Wang, *J. Alloys Compd.*, 2021, **865**, 158864.
5. F. Luo, L. Guo, Y. Xie, J. Xu, W. Cai, K. Qu and Z. Yang, *J. Mater. Chem. A*, 2020, **8**, 12378-12384.
6. K. Wang, B. Huang, F. Lin, F. Lv, M. Luo, P. Zhou, Q. Liu, W. Zhang, C. Yang, Y. Tang, Y. Yang, W. Wang, H. Wang and S. Guo, *Adv. Energy Mater.*, 2018, **8**, 1801891.
7. J. Q. Chi, X. J. Zeng, X. Shang, B. Dong, Y. M. Chai, C. G. Liu, M. Marin and Y. Yin, *Adv. Funct. Mater.*, 2019, **29**, 1901790.
8. F. Yang, Y. Zhao, Y. Du, Y. Chen, G. Cheng, S. Chen and W. Luo, *Adv. Energy Mater.*, 2018, **8**, 1703489.
9. N. Zhang, Q. Shao, Y. Pi, J. Guo and X. Huang, *Chem. Mater.*, 2017, **29**, 5009-5015.
10. N. Jia, Y. Liu, L. Wang, P. Chen, X. Chen, Z. An and Y. Chen, *ACS Appl. Mater. Interfaces*, 2019, **11**, 35039-35049.
11. J. Yu, G. Li, H. Liu, L. Zhao, A. Wang, Z. Liu, H. Li, H. Liu, Y. Hu and W. Zhou, *Adv. Funct. Mater.*, 2019, **29**, 1901154.
12. Q. Qian, J. Zhang, J. Li, Y. Li, X. Jin, Y. Zhu, Y. Liu, Z. Li, A. El-Harairy, C. Xiao, G. Zhang

- and Y. Xie, *Angew. Chem., Int. Ed.*, 2021, **60**, 5984-5993.
13. Y. Liu, J. Zhang, Y. Li, Q. Qian, Z. Li, Y. Zhu and G. Zhang, *Nat. Commun.*, 2020, **11**, 1853.
14. C. Zhang, H. Liu, Y. Liu, X. Liu, Y. Mi, R. Guo, J. Sun, H. Bao, J. He, Y. Qiu, J. Ren, X. Yang, J. Luo and G. Hu, *Small Methods*, 2020, **4**, 2000208.
15. Y. Li, J. Li, Q. Qian, X. Jin, Y. Liu, Z. Li, Y. Zhu, Y. Guo and G. Zhang, *Small*, 2021, **17**, 2008148.
16. Z. Wang, L. Xu, F. Huang, L. Qu, J. Li, K. A. Owusu, Z. Liu, Z. Lin, B. Xiang, X. Liu, K. Zhao, X. Liao, W. Yang, Y. B. Cheng and L. Mai, *Adv. Energy Mater.*, 2019, **9**, 1900390.
17. Q. Sun, M. Zhou, Y. Shen, L. Wang, Y. Ma, Y. Li, X. Bo, Z. Wang and C. Zhao, *J. Catal.*, 2019, **373**, 180-189.
18. J. Y. Zhang, H. Wang, Y. Tian, Y. Yan, Q. Xue, T. He, H. Liu, C. Wang, Y. Chen and B. Y. Xia, *Angew. Chem., Int. Ed.*, 2018, **57**, 7649-7653.
19. C. Tang, R. Zhang, W. Lu, Z. Wang, D. Liu, S. Hao, G. Du, A. M. Asiri and X. Sun, *Angew. Chem., Int. Ed.*, 2017, **56**, 842-846.
20. P. Babar, A. Lokhande, V. Karade, I. J. Lee, D. Lee, S. Pawar and J. H. Kim, *J. Colloid Interface Sci.*, 2019, **557**, 10-17.